Fluorescence Lifetime and Anisotropy Studies with Liver Alcohol Dehydrogenase and Its Complexes†

Maurice R. Eftink* and Karen A. Hagaman‡
Department of Chemistry, University of Mississippi, University, Mississippi 38677
Received March 18, 1986; Revised Manuscript Received June 23, 1986

ABSTRACT: From measurements of the apparent phase and modulation fluorescence lifetime of liver alcohol dehydrogenase at multiple modulation frequencies (6, 18, and 30 MHz), the individual lifetimes and fractional intensities of Trp-314 and Trp-15 are calculated. Values of $\tau_{314} = 3.6$, $\tau_{15} = 7.3$, and $f_{314} = 0.56$, at 20 °C, are found. These values are in general agreement with values previously reported by Ross et al. [Ross, J. B. A., Schmidt, C. J., & Brand, L. (1981) *Biochemistry 20*, 4369] using pulse-decay methodology. In ternary complexes formed between the enzyme, NAD^+ and either pyrazole or trifluoroethanol, the fluorescence lifetime of Trp-314 is found to be reduced, indicating that the binding of these ligands causes a dynamic quenching of this residue. The lifetime of Trp-314 is decreased more in the trifluoroethanol ternary complex than that with pyrazole. Also, the alkaline quenching transition of alcohol dehydrogenase is found to result in the selective, dynamic quenching of Trp-314. No change in the lifetimes of the two Trp residues is found upon selective removal of the active-site zinc atoms. From studies of the fluorescence anisotropy, r, of the enzyme as a function of added acrylamide (which selectively quenches the surface Trp-15 residue), the steady-state anisotropy of each residue is determined to be $r_{314} = 0.26$ and $r_{15} = 0.21$. In the ternary complexes the anisotropy of each residue increases slightly. The increase in r_{314} is expected, since its lifetime is reduced upon NAD^+ binding, but the increase in r_{15} indicates that the motional freedom of Trp-15 is limited by the binding of ligands, even though this residue is far from the active site.

The two types of tryptophanyl residues in the dimeric protein horse liver alcohol dehydrogenase (LADH)[1] have distinctly different fluorescence properties. These residues thus serve as intrinsic reporter groups for investigating changes in the conformation of the protein. Trp-15 is located at the surface of LADH, has a red-shifted fluorescence spectrum, and is accessible to solute quenchers such as iodide, acrylamide, and molecular oxygen (Brändén et al., 1975; Abdallah et al., 1978; Laws & Shore, 1978; Eftink & Selvidge, 1982; Eftink & Jameson, 1982; Ross et al., 1981). Trp-314 is located in an apolar environment at the intersubunit interface of the protein. Its fluorescence spectrum is blue-shifted and it is relatively inaccessible to solute quenchers. The rate constant for quenching Trp-314 by the polar quencher acrylamide is found to be, at most, one-hundredth the value for Trp-15 (Eftink & Selvidge, 1982). For the smaller and less polar quencher, oxygen, the quenching rate constant for Trp-314 is found to be about one-eighth the value for Trp-15 (Eftink & Jameson, 1982; Hagaman & Eftink, 1984). The deep burial of Trp-314 is further evidenced by the observation of room temperature phosphorescence of this residue in oxygen-depleted solutions (Saviotti & Galley, 1974; Calhoun et al., 1983).

In this paper we will take advantage of the distinctive fluorescence properties of these residues to probe changes in the protein upon ligand binding. The formation of a ternary complex with the coenzyme NAD^+ and the inhibitor trifluoroethanol (TFE) results in a large drop in the fluorescence of the protein, apparently due to selective quenching of Trp-314 (Laws & Shore, 1978; Eftink & Selvidge, 1982). A ternary complex formed with the inhibitor pyrazole also quenches the fluorescence of the protein, although to a lesser extent than in the TFE complex (Theorell & Tatemoto, 1971; Eftink, 1986; Ross et al., 1981). Here we will use fluorescence lifetime, quenching, and anisotropy measurements to characterize changes in the microenvironment of the two types of tryptophanyl residues upon formation of these complexes. Also we will study changes accompanying the alkaline transition of LADH and the removal of the active-site zinc ions to form apo-LADH. The alkaline transition (controlled by a pK_a of ~9.6) also causes a quenching of the fluorescence of the protein, due to selective quenching of Trp-314 (Wolfe et al., 1977; Laws & Shore, 1978; Eftink, 1986). Apo-LADH, prepared by the method of Maret et al. (1979), has been used in recent years to investigate the role of the active-site zinc in the kinetics and thermodynamics of coenzyme binding; a characterization of the fluorescence of apo-LADH should provide evidence regarding whether its solution structure is similar to that of LADH.

We will use multifrequency phase/modulation fluorescence lifetime measurements to dissect the component lifetimes of the two types of tryptophanyl residues. The capacity of this technique to analyze heterogeneously decaying systems has been discussed elsewhere (Gratton et al., 1984; Jameson et al., 1984). Fluorescence anisotropy measurements will be made as a function of added quencher, acrylamide, in order to resolve the individual anisotropy components of the two tryptophanyl residues (Eftink, 1983). The anisotropy values, together with the lifetime values of the residues, will provide information about the rotational mobility of the residues in the free protein and the ternary complexes.

Experimental Procedures

Materials. NAD^+ (lithium salt) and LADH were obtained from Calbiochem-Behring. The protein was a suspension of

† This work was supported by National Science Foundation Grants PCM 82-06073 and DMB-8511569.
‡ Present address: Merrell Dow Research Institute, Cincinnati, OH 45215.

[1] Abbreviations: LADH, horse liver alcohol dehydrogenase; NAD^+, oxidized nicotinamide adenine dinucleotide; TFE, trifluoroethanol.

0006-2960/86/0425-6631$01.50/0

Table I: Analysis of Apparent Phase and Modulation Fluorescence Lifetimes of Indole Mixtures[a]

mixtures	τ_p (ns); τ_m (ns)			fits	
	6 MHz	18 MHz	6 MHz	Weber's algorithm[c]	least squares[c]
2-methylindole (τ_1 = 2.40 ± 0.15 ns)[b] 3-methylindole (τ_2 = 9.57 ± 0.35 ns) f_1 = 0.40	6.61 (6.68);[d] 8.44 (8.39)	5.66 (5.60); 7.76 (7.81)	4.51 (4.53); 7.00 (7.04)	τ_1 = 1.84 τ_2 = 9.23 f_1 = 0.33	τ_1 = 1.86 τ_2 = 9.33 f_1 = 0.330
5-methylindole (τ_1 = 2.93 ± 0.11 ns) 3-methylindole (τ_2 = 9.57 ± 0.35 ns) f_1 = 0.62	5.10 (5.07); 6.64 (6.61)	4.34 (4.39); 5.84 (5.84)	3.93 (3.91); 5.17 (5.14)	τ_1 = 2.92 τ_2 = 9.19 f_1 = 0.63	τ_1 = 2.92 τ_2 = 9.22 f_1 = 0.635
indole (τ_1 = 4.70 ± 0.17 ns) 3-methylindole (τ_2 = 9.57 ± 0.35 ns) f_1 = 0.55	7.07 (7.05); 8.44 (7.83)	6.43 (6.55); 7.27 (7.32)	6.27 (6.22); 7.08 (6.94)	τ_1 = 4.48 τ_2 = 9.23 f_1 = 0.35	τ_1 = 4.94 τ_2 = 9.78 f_1 = 0.541
2-methylindole (τ_1 = 2.40 ± 0.15 ns) indole (τ_2 = 4.70 ± 0.17 ns) f_1 = 0.32	3.70 (3.68); 4.06 (4.02)	3.61 (3.59); 4.02 (3.96)	3.46 (3.47); 3.84 (3.86)	τ_1 = 2.64 τ_2 = 5.12 f_1 = 0.57	τ_1 = 2.10 τ_2 = 4.50 f_1 = 0.337

[a] Conditions: 20 °C; excitation at 295 nm; emission at 350 nm; solutions not degassed. [b] Lifetimes of the pure components are averages of the phase and modulation lifetimes at 6, 18, and 30 MHz. [c] The Weber's algorithm fit for the data at 6 and 30 MHz; the least-squares fit is for all three frequencies. [d] The values in parentheses are calculated values using the τ_1, τ_2, and f_1 from the least-squares fit.

crystals in 10% ethanol and was dialyzed vs. three changes of buffer (0.01 M sodium monobasic phosphate, 0.02 M sodium dibasic phosphate, pH 7.2) in the cold before use. Pyrazole was recrystallized from cyclohexane. Acrylamide was recrystallized from ethyl acetate. TFE and dipicolinic acid were obtained from Sigma Chemical Co. Indole, 2-methylindole, 3-methylindole, and 5-methylindole were sublimed before use.

Apo-LADH was prepared according to the procedure of Maret et al. (1979). The apo-LADH samples used in our fluorescence studies had a residual enzymatic activity of ~5% (by the assay of Dalziel (1957)). All protein samples were passed through a millipore filter before fluorescence measurements were made.

Methods. Steady-state acrylamide quenching studies were performed as described elsewhere (Eftink & Selvidge, 1982) in order to obtain f_i, the fractional contribution of the two classes of tryptophanyl residues to the total fluorescence intensity, and $K_{sv,i}$, the Stern–Volmer quenching constants for each class of residue. Equation 2 of Eftink and Selvidge (1982) was used to analyze such data. Static quenching was ignored in the fits. Either a Perkin-Elmer MPF 44A or a SLM 4800 (in the steady-state mode) spectrophotofluorometer was used for measuring fluorescence intensity. Temperature-jacketed cell holders were used and the temperature of the solutions in the cells was measured with a Digitec 5810 digital thermometer.

Fluorescence anisotropy, r, measurements were made with the Perkin-Elmer fluorometer, using HBN Polaroid polarizers, as described in Eftink (1983). An excitation wavelength of 300 nm (5-nm bandwidth) was used. Emission was observed at 323 nm (10-nm bandwidth).

Apparent phase and modulation fluorescence lifetimes τ_p and τ_m were measured with the SLM 4800 fluorometer. An excitation wavelength of 295 nm was used (0.5-nm bandwidth) and emission was observed through a Corning 7-60 filter. A glycogen suspension was used as reference.

Phase angle and modulation data were analyzed to obtain τ_i and f_i values using eq 32–35 of Weber 1981). Data at 6 and 30 MHz were used in the analysis. Alternatively, a least-squares analysis, as outlined by Jameson et al. (1984), was employed.

Results

Heterogeneity Analysis of Indole Mixtures. Indole, 2-methylindole, 3-methylindole, and 5-methylindole were found to have fluorescence lifetimes of 4.7, 2.4, and 9.6, and 2.9 ns, respectively, at 20 °C. For each fluorophore, the lifetimes are independent of modulation frequency (measurements at 6, 8, and 30 MHz) and the τ_p and τ_m agree within 5% at each frequency. Thus the emission of these compounds is a single-exponential decay process (Gratton et al., 1984; Jameson et al., 1984).

Binary mixtures of indole and the various methylindoles were prepared. Apparent phase and modulation lifetimes were measured for these mixtures at 6, 18, and 30 MHz. The data are given in Table I. Analysis via the algorithm of Weber (1981) for a binary system resulted in the resolution of the component lifetime and fractional intensity values also shown in Table I (using 6- and 30-MHz data). As can be seen, the resolved τ_i and f_i are usually within 10% of the expected values for the components. With the data at all three frequencies and a least-squares algorithm, a slight improvement in the resolution of the components is achieved (Jameson & Gratton, 1983). These studies with indole mixtures demonstrate the ability of multifrequency phase/modulation fluorometry, in our hands, to resolve the parameters for a binary fluorescence decay. The commercial instrument that we used operates at three modulation frequencies. Instrumentation has recently been developed that enables a larger number and range of frequencies to be used in the UV range (Jameson et al., 1984; Lakowicz & Maliwal, 1985). Multifrequency measurements with this new technology should improve the ability of this method to resolve components.

Heterogeneity Analysis for LADH and Its Complexes. The apparent phase and modulation lifetimes of LADH were measured at modulation frequencies of 6, 18, and 30 MHz at a temperature of 20 °C. The measured τ_p and τ_m showed much greater variation from day to day (i.e., for different preparations) than the indole solutions. For this reason and due to the variabilities intrinsic to the tuning of the phase/modulation fluorometer (Jameson et al., 1984), we report in Table II average values for 19 separate determinations. In spite of the large standard deviations, particularly for the τ_m at 6 MHz, the resolved τ_i values obtained by analysis via Weber's algorithm are in excellent agreement with previously reported lifetime values for LADH. The f_i values obtained correspond to broad-band emission through a Corning 7-60 filter, and, since there is a wavelength dependence of the preexponential factors for τ_1 and τ_2, our f_i cannot be simply related to the preexponentials found by Ross et al. (1981). As shown below, independent determinations of the f_i values by selective acrylamide fluorescence quenching are in support of

Table II: Phase and Modulation Lifetime Data and Component Lifetimes for LADH[a]

	6 MHz	18 MHz	30 MHz
τ_p	5.19 ± 0.13 (5.21)	4.92 ± 0.19 (4.93)	4.67 ± 0.15 (4.68)
τ_m	5.83 ± 0.38 (5.81)	5.50 ± 0.27 (5.54)	5.24 ± 0.12 (5.25)

ref	f_1	τ_1	f_2	τ_2
this work	0.56	3.64	0.44	7.33
Ross et al. (1981)[b]		3.8		7.0
Eftink and Jameson (1982)[c]		3.6		6.9
Beechem et al. (1983)[d]		3.95		7.45
Beechem et al. (1983)[e]		3.75		7.09

[a] Lifetimes in nanoseconds. Data at 20 °C, unless stated otherwise. The τ_p and τ_m given are the average of 18 determinations for different days and/or sample preparations. The τ_p and τ_m values given in parentheses are calculated values for the fit, via Weber's algorithm (6- and 30-MHz data), for $\tau_1 = 3.64$, $\tau_2 = 7.33$, and $f_1 = 0.56$. A nonlinear least-squares, analysis yielded a nearly identical fit: $\tau_1 = 3.60$, $\tau_2 = 7.27$, and $f_1 = 0.55$. [b] Pulse/decay lifetime measurement at 27.5 °C. [c] Phase lifetime measurement with selective acrylamide quenching at 20 °C. [d] Phase/modulation measurements with global analysis at 20 °C. [e] Pulse/decay measurement at 18.5 °C.

the resolved values. (We have very recently updated our fluorometer, with a Pockels cell modulator obtained from ISS, Inc., Champaign, IL, so that it will operate over a continuous-frequency range of 1–200 MHz. Using this new equipment, along with the lifetime distribution analysis developed by Gratton and co-workers (Alcala et al., 1986), we have confirmed that the fluorescence decay of LADH is characterized by two lifetimes, a short one centered at about 3.3 ns and a long one centered at about 6.5 ns).

Previous fluorescence lifetime studies (Ross et al., 1981; Eftink & Jameson, 1982) have clearly demonstrated that the lifetimes of 3.6 and 7.3 ns can be assigned to emission from Trp-314 and Trp-15, respectively.

The phase/modulation heterogeneity analysis was also performed with data for two ternary complexes, LADH–NAD^+–TFE and LADH–NAD^+–pyrazole. As shown in Table III, τ_2, the lifetime of Trp-15, does not change when these ligands bind. The lifetime of Trp-314, τ_1, decreases to 2.1 and 1.4 ns in the pyrazole and TFE ternary complexes, respectively. This indicates that dynamic quenching of Trp-314 occurs upon binding coenzyme plus inhibitor and that a greater degree of quenching occurs in the TFE complex. Ross et al. (1981) have previously reported lifetimes of 2.4 and 7.2 ns for Trp-314 and Trp-15 in the LADH–NAD^+–pyrazole complex (at 10 °C). Note also that we find drops in f_1 (and increases in f_2) concomitant with the decreases in τ_1. This is also consistent with dynamic quenching of Trp-314. Note that a small extent of static quenching of Trp-15 cannot be excluded by this data. The drops in f_1 are less than expected from the decreases in τ_1, which could be due to the fact that there is a "static" loss in intensity from Trp-15 upon complex formation as well. Previous decay studies by Knutson et al. (1982) have also suggested this possibility.

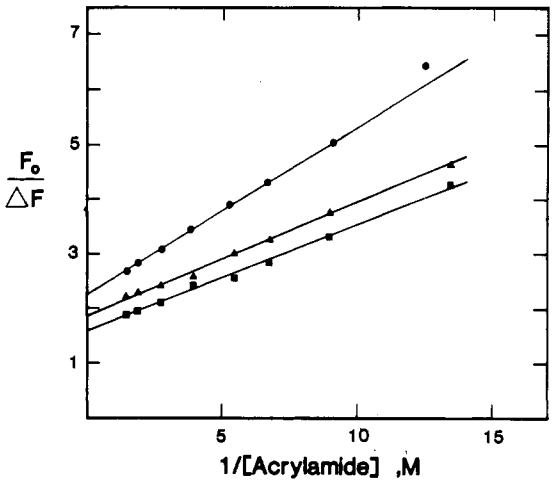

FIGURE 1: Modified Stern–Volmer plot for the quenching of the fluorescence of LADH (●), the LADH–NAD^+–pyrazole ternary complex (▲), and the LADH–NAD^+–TFE ternary complex (■) by acrylamide. (See Eftink & Ghiron (1981) and Eftink & Selvidge (1982) for an explanation of this plot.) Conditions: 20 °C, pH 7.2 phosphate buffer, λ_{ex} = 295 nm, emission through a corning 7-60 filter, 5×10^{-5} M NAD^+ plus either 2.5×10^{-3} M pyrazole or 1.8×10^{-2} M TFE.

At pH 10.55, where the alkaline quenching transition is 85% completed, the lifetime and fractional intensity of Trp-314 both are smaller than at neutral pH. Again the lifetime of Trp-15 appears unchanged. In this case the decreases in f_1 and τ_1 are consistent with pure dynamic quenching of Trp-314 (i.e., no static quenching of either type of tryptophanyl residue). Since LADH is unstable at pH >10 (DeTraglia et al., 1977) these experiments were performed by making phase and modulation measurements within a few minutes after the addition of a 0.05 M Na_2CO_3 buffer solution (at pH 10.8) to an unbuffer protein solution. For each frequency, fresh protein solutions were used.

τ_i and f_i values for apo-LADH, in which the active-site Zn^{2+} ions have been selectively removed, were found to be nearly the same as those for LADH. Since fewer data sets were taken for apo-LADH, the small differences reported in Table III are not deemed significant.

Steady-State Acrylamide Quenching Studies. The ability of acrylamide to selectively quench the fluorescence of the surface residue Trp-15 was used to independently determine the fractional fluorescence contributions, f_i, of each type of residues (Eftink & Selvidge, 1982). Since the fluorescence contributions are quite dependent on both emission and excitation wavelength (and hence to a certain extent on bandwidths), the acrylamide quenching method was used to determine f_i values for the different conditions and instruments (e.g., emission filters were used for the above lifetime measurements; an emission monochromater was used for the anisotropy studies). Also, of course, this method was used to determine f_i for the LADH ternary complexes, high pH, and apo forms of LADH.

Table III: Phase and Modulation Fluorescence Lifetime Analysis for LADH and LADH Complexes and Acrylamide Quenching Parameters[a]

	phase/modulation lifetime analysis				acrylamide quenching parameters			
	f_1	τ_1 (ns)	f_2	τ_2 (ns)	f_{314}	f_{15}	$K_{sv,15}$ (M^{-1})	$k_{q,15}$ (10^{-9} M^{-1} s^{-1})
LADH	0.56	3.64	0.44	7.33	0.56	0.44	7.3	1.0
LADH–NAD^+–TFE	0.35	1.43	0.65	6.98	0.38	0.62	8.3	1.2
LADH–NAD^+–pyrazole	0.54	2.13	0.46	7.12	0.48	0.52	9.5	1.3
LADH, pH 10.55[b]	0.42	2.22	0.58	7.00	0.41	0.59	6.5	0.9
apo-LADH	0.66	3.26	0.34	8.03	0.60	0.40	6.1	0.8

[a] Conditions: pH 7.2 sodium phosphate buffer, 20 °C; λ_{ex} = 295 nm, emission through a Corning 7-60 filter. Phase/modulation data analyzed via Weber's algorithm to obtain τ_i and f_i. Steady-state acrylamide quenching studies performed on SLM fluorometer with same λ_{ex} and emission filter. [b] 0.1 M NaCl solution with an aliquot of 0.05 M Na_2CO_3 added to bring final pH to 10.55. Phase and modulation lifetime measurements made within 10 min of pH jump.

Table IV: Steady-State Acrylamide Quenching Parameter for LADH and LADH Complexes under the Conditions Used for Anisotropy Studies[a]

	f_{15}	$K_{sv,15}$ (M^{-1})	$k_{q,15}$ (10^{-9} M^{-1} s^{-1})
LADH	0.31	8.2	1.1
LADH–NAD^+–pyrazole	0.43	7.3	1.0
LADH–NAD^+–TFE	0.52	7.2	1.0

[a] Conditions: λ_{ex} = 300 nm, λ_{em} = 340 nm, 25 °C, pH 7.2 sodium phosphate buffer. $k_{q,15}$ values calculated from the $K_{sv,15}$ and the fluorescence lifetimes for Trp-15 given in Table III.

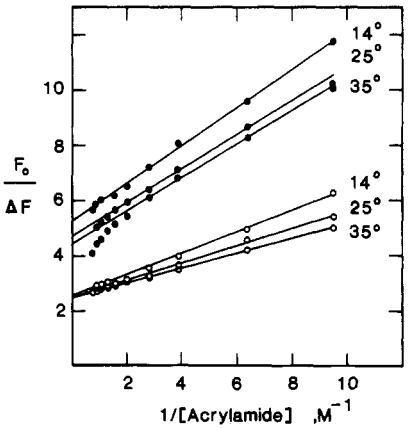

FIGURE 2: Modified Stern–Volmer plot for the acrylamide quenching of the fluorescence of LADH (●) and the LADH–NAD^+–TFE ternary complex (○) as a function of temperature.

In Figure 1 are shown modified Stern–Volmer plots for LADH and its ternary complexes with NAD^+–pyrazole and NAD^+–TFE, using the instrument and conditions employed for the lifetime measurements in Table III. The fractional intensities of Trp-15 (obtained as the inverse of the intercept of the lines in Figure 1) and Trp-314 are listed in Table III. As seen for these data, as well as for that for LADH at pH 10.8 and apo-LADH, the values of f_{314} and f_{15} obtained independently from the acrylamide steady-state quenching experiment are in excellent agreement with the f_1 (=f_{314}) and f_2 (=f_{15}) values found in the lifetime heterogeneity analysis experiments.

From the values of the Stern–Volmer quenching constant, K_{sv}, found for each case, along with the fluorescence lifetime of Trp-15, were calculated the values for the rate constant, $k_{q,15}$, for acrylamide quenching of Trp-15 (i.e., $K_{sv} = k_q\tau_0$, where τ_0 is an unquenched fluorescence lifetime). As seen in Table III, $k_{q,15}$ is approximately the same for LADH under all conditions studied.

Steady-state acrylamide quenching data, performed in conjunction with the fluorescence anisotropy studies to be presented below, yielded the f_i values given in Table IV.

The temperature dependence of the acrylamide quenching of LADH and the LADH–NAD^+–TFE ternary complex was also studied, as shown in Figure 2. The modified Stern–Volmer plots for the ternary complex are almost perfectly linear at temperature ranging from 14 to 35 °C. For LADH, the plots deviate from linearity at high quencher concentration. These deviations are due to the fact that the acrylamide quenching constant for Trp-314 is not zero (Eftink & Ghiron, 1981). As we argued earlier (Eftink & Selvidge, 1982), in order to fit the acrylamide quenching data for LADH, a quenching constant of 0.04 must be included for Trp-314 (compared to $K_{sv} \approx 10$ M^{-1} for Trp-15). The fact that the slight curvature at high quencher concentration is more pronounced at higher temperature indicates that the activation

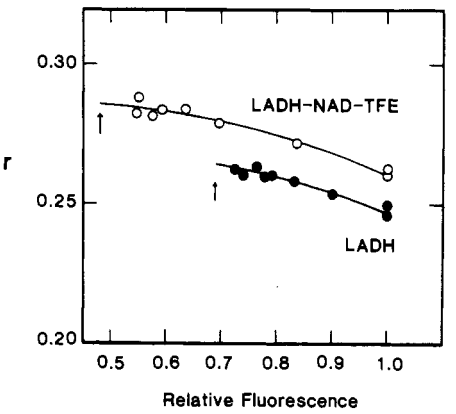

FIGURE 3: The steady-state anisotropy, r, of LADH and the LADH–NAD^+–TFE ternary complex as a function of the fluorescence (λ_{ex} = 300 nm; λ_{em} = 340 nm) unquenched by acrylamide. The arrow marks the fluorescence intensity, due to Trp-314, that is approached at high acrylamide quencher concentration.

Table V: Steady-State Anisotropy of Trp-314 and Trp-15 of LADH and LADH Complexes[a]

	r_i	$\tau_{0,i}$ (ns)	ϕ_i (ns)
LADH			
Trp-314	0.265	3.6	21
Trp-15	0.210	7.3	15
LADH–NAD^+–TFE			
Trp-314	0.290	1.4	20
Trp-15	0.235	7.0	22
LADH–NAD^+–pyrazole			
Trp-314	0.285	2.1	24
Trp-15	0.235	7.1	22

[a] Assuming r_0 = 0.31.

enthalpy for the acrylamide quenching of Trp-314 is large. From the apparent absence of a deviation at high quencher concentrations for the ternary complex we can conclude that the rate constant for acrylamide quenching of Trp-314 in the complex is even smaller than in the free protein.

Quenching Resolved Emission Anisotropy (QREA) Studies. The steady-state emission anisotropy, r, of LADH and the ternary complexes was measured as a function of added quencher, acrylamide, as shown in Figure 3. The value of r is a weighted average; i.e., $r = \sum f_i r_i$, where r_i is the anisotropy of each type of tryptophanyl residue. Since acrylamide selectively quenches the fluorescence of the surface residue, Trp-15, the limiting r value approached at high quencher concentration, [Q], will be approximately that of Trp-314 (Eftink, 1983). For LADH, the r values at zero, $r(0)$, and high [Q], $r(Q)$, are 0.245 and 0.265, respectively. Assigning $r(Q) = r_{314} = 0.265$ and by using f_{15} and f_{314} values determined independently from acrylamide quenching data under identical conditions (i.e., 300-nm excitation wavelength, 323-nm emission wavelength), we can calculate r_{15} as $r_{15} = (r(0) - f_{314}r_{314})/f_{15} = 0.210$. Thus, from these quenching resolved emission anisotropy experiments, we find that the anisotropy of Trp-314 is much higher than that of Trp-15, as listed in Table V.

For the pyrazole and TFE ternary complexes, the anisotropy (in the absence of acrylamide) is increased to 0.263 and 0.262, respectively. Again, the addition of acrylamide leads to a further increase in r. Analyzing the data in Figure 3 in the above manner, we obtain the r_{314} and r_{15} values listed in Table V. As can be seen, upon forming the ternary complexes there is an increase in the anisotropy of both Trp-314 and Trp-15.

Discussion

The fluorescence lifetimes determined here for the two types of tryptophanyl residues of LADH by multiple frequency

phase/modulation fluorometry are in excellent agreement with the values determined previously by using pulse-decay methodology (Ross et al., 1981; Knutson et al., 1982; Beechem et al., 1983) and a quenching resolved lifetime analysis (Eftink & Jameson, 1982). Beechem et al. (1983) have also recently reported similar lifetimes using a global analysis of multiple frequency phase/modulation data. The arguments leading to the assignment of τ_1 and τ_2 to the lifetimes of Trp-314 and Trp-15, respectively, are given in the previous studies (Ross et al., 1981; Eftink & Jameson, 1983).

Trp-314 in LADH can thus be characterized as having a blue-shifted fluorescence, as having a red-shifted excitation spectrum, as having a fluorescence lifetime of 3.6 ns, as having an anisotropy of 0.265 (with 300-nm excitation), and as being relatively inaccessible to quenchers. From the estimated quantum yield of 0.31–0.37 for this residue (Abdallah et al., 1978; Knutson et al., 1982), the natural lifetime of this residue is calculated to be 10–12 ns. This natural lifetime is comparable to that found for 3-methylindole in cyclohexane (Meech et al., 1983; Szabo et al., 1983). In previous work we have argued that the rate constant for acrylamide quenching of Trp-314 is $\leq 10^7$ M^{-1} s^{-1}, characterizing this residue as being one of the most deeply buried tryptophanyl residues in a protein studied to date (Eftink & Selvidge, 1982). The present studies of the temperature dependence of acrylamide quenching further indicate that the activation enthalpy, $\Delta H^{\ddagger}$, for acrylamide quenching is large, although it is not possible to extract a value of this $\Delta H^{\ddagger}$. Large $\Delta H^{\ddagger}$ for solute quenching have been related to the magnitude for structural/enthalpy fluctuations in proteins that are required for the inward penetration of a quencher to a buried fluorophore (Eftink & Ghiron, 1975, 1977, 1981). We have determined a $\Delta H^{\ddagger}$ of 10–12 kcal/mol for the oxygen quenching of the fluorescence of Trp-314 (Hagaman & Eftink, 1984). This $\Delta H^{\ddagger}$ is large for the quencher oxygen (the latter, being smaller than other quenchers such as acrylamide, should require smaller structural fluctuations for diffusion through a globular protein). Thus, while oxygen can quench Trp-314 with a rate constant that is 5–10% of the diffusion-controlled rate constant, the large $\Delta H^{\ddagger}$ indicates that the oxygen must penetrate deeply into the protein to strike Trp-314 and that this penetration involves a dynamic response of the protein.

When NAD^+ and TFE are bound to the protein, the rate constant for acrylamide quenching of Trp-314 is apparently further decreased. This suggests that the binding of ligands further limits (the already infrequent) fluctuations in the protein in the vicinity of Trp-314.

The formation of both the LADH–NAD^+–TFE and LADH–NAD^+–pyrazole ternary complexes results in the dynamic quenching of Trp-314, with more quenching occurring in the TFE complex. The mechanism of the quenching of Trp-314 is uncertain. Ross et al. (1981) and Abdallah et al. (1979) have considered the possibility that Forster energy transfer occurs between Trp-314 and the bound coenzyme. As we have argued in a preceding paper (Eftink, 1986), the quenching of Trp-314 produced by NAD^+ and inhibitor binding does not appear to be due to a shift in the alkaline quenching effect to lower pH. X-ray crystallographic studies do not reveal any significant differences in the positioning of amino acid side chains around Trp-314 on comparison of the structure of LADH with its ternary complexes (Brändén et al., 1975; Brändén & Eklund, 1978). Thus, unless a very subtle structural changes occurs to bring a quenching group into dynamic proximity of Trp-314, the energy-transfer mechanism seems to be the most reasonable possibility. However, it is not clear why there is more quenching of Trp-314 on forming the TFE ternary complex as compared to the pyrazole ternary complex. On forming the latter complex it is known that there is an increase in absorbance at ~300 nm (presumably a perturbation of the bound NAD^+ spectrum) (Theorell & Yometani, 1963) that would favor energy-transfer quenching. However, there appears to be a much smaller perturbation in the spectrum of bound NAD^+ in the TFE ternary complex (Eftink, unpublished result) and thus it is not clear why there is more quenching in this complex. Slight differences in the relative orientation of the indoyl donor and nicotinamide acceptor groups may account for the differences in quenching of the two ternary complexes.

Trp-15 has a red-shifted fluorescence spectrum, has a blue-shifted excitation spectrum, has a fluorescence lifetime of 7.3 ns, has an anisotropy of 0.21, and is relatively accessible to solute quenchers. From the quantum yield of 0.19–0.25 for this residue (Abdallah et al., 1979; Knutson et al., 1982) is calculated a natural lifetime of 29–38 ns. This can be compared to natural lifetimes of 25.3–32.7 ns found for 3-methylindole in aqueous solution (Szabo et al., 1983; Meech et al., 1983) and is consistent with the notion that the indole ring of Trp-15 is solvent exposed and is able to undergo dipolar relaxation with solvent and polar amino acid side chains in its microenvironment.

The fluorescence lifetime of Trp-15 is unchanged upon the formation of the ternary complexes or as a result of the alkaline transition. The observation that f_{314} does not decrease (and f_{15} does not increase) to the extent expected from the drop in τ_{314} upon ternary complex formation is consistent with the observed drop in the preexponential factor, α_{15}, for Trp-15 in fluorescence decay experiments upon complex formation (Knutson et al., 1983) and suggests that Trp-15 is statically quenched.[2] The basis for such static quenching is uncertain. As will be mentioned below, the crystal structure of LADH ternary complexes shows a slight change in the microenvironment of Trp-15 from that in the absence of ligands.

The fluorescence anisotropy values for the tryptophanyl residues, r_i, can be related to their fluorescence lifetimes (in the absence of quencher), τ_{oi}, and rotational correlation times for isotropic motion of the indole ring, ϕ_i, according to the Perrin equation

$$r_i = r_0/(1 + \tau_{oi}/\phi_i) \quad (1)$$

where r_0 is the anisotropy in the complete absence of motion. In our previous work we found $r_0 = 0.31$ to be appropriate for the indole fluorophore (with an excitation wavelength of 300 nm) (Eftink, 1983). The rotational motion of indole side chains of proteins will usually not be described by a single isotropic rotational correlation time. The indole ring will be depolarized by the global rotation of the protein, with rota-

[2] Ross et al. (1981) have previously reported a rotational correlation time of 36 ns (at 27.5 °C) for LADH by anisotropy decay measurements. A single-exponential anisotropy decay was observed, so they concluded that both Trp residues have the above rotational correlation time. Our apparent ϕ for Trp-314 is smaller than, but not in discord with, the value of Ross et al. This is because our apparent ϕ includes a contribution from any rapid, subnanosecond segmental motion, as well as slower global rotation of the protein. The value determined by Ross et al. likely reflects the slowest depolarizing motions; subnanosecond motion may go undetected by this method. If the value of 36 ns more correctly describes the global rotation of Trp-314, then our value of $r_{314} = 0.265$ indicates that very rapid segmented motion of Trp-314 with a cone angle, θ, of ~10° also occurs. That is, Trp-314 may not be completely immobilized with the enzyme, but, on comparison to the θ of Trp residues in other single-Trp proteins (Eftink, 1983), it is clear that Trp-314 must be characterized as having limited segmental mobility.

tional correlation time ϕ_2, and by local, independent rotation of the side chain, with rotational correlation time ϕ_1. As we observed for several single tryptophan containing proteins, ϕ_1 is usually much smaller than ϕ_2, so that the apparent ϕ from eq 1 (i.e., the apparent ϕ determined by anisotropy decay or QREA experiments) will reflect primarily ϕ_2, and the existence of rapid segmental motion will be revealed by an apparent r_0 that is less than the value of $r_0 = 0.31$. The ratio $r_0(\text{app})/r_0$ can be interpreted in terms of a cone angle, θ, within which the side chain rapidly rotates (Weber, 1952; Gottlieb & Wahl, 1963; Lakowicz et al., 1982).

$$r_0(\text{app})/r_0 = (3\cos^2\theta - 1)/2 \qquad (2)$$

The value of $r_{314} = 0.265$ for Trp-314 in LADH is a relatively large anisotropy value for a tryptophanyl residue in a protein at room temperature (Eftink, 1983). Using $\tau_{314} = 3.6$ ns and $r_0 = 0.31$, we calculate an apparent ϕ of 21 ns from eq 1. This value is almost equal to the value of 29 ns that is theoretically predicted for the rotational correlation time of a spherical protein of molecular weight 80000 Da (Eftink, 1983, eq 3). Since LADH has an asymmetric shape (approximating a prolate ellipsoid of 2:1 axial ratio), it rotates anisotropically, and, depending on the angle between the long axis of the protein and the emission oscillator of the indole ring, the effective rotational correlation time for global rotation of the protein may be greater than or less than the above value of 29 ns for rotation of a spherical protein.[2] Furthermore, the large value of r_{314} (and the fact the difference between r_{314} and r_0 can be reasonably explained in terms of depolarization due to global rotation of the protein) argues that resonance energy transfer between the two trp-314 residues in the dimeric protein does not occur to a significant extent, at least when the excitation wavelength is 300 nm. The two Trp-314 residues in LADH are relatively close to one another (~6 Å separation) (Eklund et al., 1976), and if energy transfer were to occur between these residues it would be expected to result in a depolarization of the emission (Grinvald & Steinberg, 1974; Ghiron & Longworth, 1979). The apparent absence of a significant degree of Trp-314 to Trp-314 energy transfer at $\lambda_{ex} = 300$ nm is consistent with the red-edge repolarization effect previously demonstrated by Weber and Shinitzky (1970).

From r_{15} and τ_{15}, an apparent rotational correlation time of 15 ns is calculated for Trp-15. This value is significantly lower than the expected rotational correlation time for global rotation of the protein and indicates that rapid, independent motion of the indole ring of this residue occurs. It is impossible from these data to determine the time scale of this rapid motion. However, if one assumes that the Trp-15 undergoes rapid segmental motion over a limited cone angle and slower depolarization due to global rotation of the protein (with $\phi_2 = 21$ ns, as is the case for Trp-314), one can calculate that this would correspond to an $r_0(\text{app})$ of 0.25, which, from eq 2 corresponds to rapid motion of Trp-15 within a cone of 14°. (If the correlation time for global rotation, ϕ_2, of 36 ns is used, as found by Ross et al. (1981), this corresponds to rapid motion of Trp-15 within a cone angle of 21°. See footnote 2.)

The binding of coenzyme, plus either pyrazole or TFE, results in an increase in the anisotropy of both Trp-15 and Trp-314. The increase in r_{314} can be explained, for both ternary complexes, as being due to the decrease in τ_{314}. After this decrease in lifetime is taken into account, apparent ϕ values of ~20–24 ns are calculated for Trp-314. These values are nearly the same as that found for this residue in the free protein, indicating that the indole side chain remains relatively immobilized within the globular protein in these complexes.

The increase in r_{15} for the ternary complexes was unexpected. Since there is no significant change in the fluorescence lifetime of this residue upon binding coenzyme and inhibitor, the apparent ϕ value increases to 22 ns for the pyrazole and TFE complexes, respectively. Thus there is an apparent restriction in the segmental motion of this residue, since the apparent ϕ for Trp-15 in the complexes is as large as the ϕ for Trp-314. This is quite surprising and interesting, particularly when one notes that Trp-15 is approximately 30 Å from the coenzyme binding site (Eklund et al., 1976). A conformational change (or attenuation in conformational dynamics) must be propagated from the coenzyme binding site through the protein matrix to the site of Trp-15 upon binding NAD^+ and inhibitor. Knutson et al. (1982) have demonstrated that the emission spectrum of Trp-15 is red-shifted upon ternary complex formation. Also, X-ray crystallographic studies have shown that the indole ring of Trp-15 has a slightly different orientation in ternary complexes, as compared to the free enzyme (Branden & Eklund, 1978). The standard enthalpy change value of −11 kcal/mol we have reported (Eftink & Byström, 1986) for the binding for pyrazole and NAD^+ to the unprotonated state of the enzyme must be considered to contain at least some contribution from an induced two-state or subtle change in the conformation of the protein (Eftink et al., 1983).

Registry No. LADH, 9031-72-5; NAD, 53-84-9; TFE, 75-89-8; L-Trp, 73-22-3; pyrazole, 288-13-1; 2-methylindole, 95-20-5; 3-methylindole, 83-34-1; 5-methylindole, 614-96-0; indole, 120-72-9.

References

Abdallah, M. A., Biellman, J. F., Wiget, P., Joppich-Kuhn, R., & Luisi, P. L. (1978) *Eur. J. Biochem. 89*, 397–405.

Alcala, J. R., Marriott, G., Gratton, E., & Prendergast, F. G. (1986) *Biophys. J. 49*, 108a.

Beechem, J. M., Knutson, J. R., Ross, J. B. A., Turner, B. W., & Brand, L. (1983) *Biochemistry 22*, 6054–6058.

Brändén, C.-I., & Eklund, H. (1978) *Excerpta Med.*, 63–80.

Brändén, C.-I., Jornvall, H., Eklund, H., & Furugren, B. (1975) *Enzymes (3rd Ed.) 11*, 103–190.

Calhoun, D. B., Vanderkooi, J. M., Woodrow, G. V., III, & Englander, S. W. (1983) *Biochemistry 22*, 1526–1532.

Dalziel, K. (1957) *Acta Chem. Scand. 11*, 397–398.

DeTraglia, M. C., Schmidt, J., Dunn, M. F., & McFarland, J. T. (1977) *J. Biol. Chem. 252*, 3493–3500.

Eftink, M. R. (1983) *Biophys. J. 43*, 323–334.

Eftink, M. R. (1986) *Biochemistry* (first of three papers in this issue).

Eftink, M. R., & Ghiron, C. A. (1975) *Proc. Natl. Acad. Sci. U.S.A. 72*, 3290–3294.

Eftink, M. R., & Ghiron, C. A. (1977) *Biochemistry 16*, 5546–5551.

Eftink, M. R., & Ghiron, C. A. (1981) *Anal. Biochem. 114*, 199–227.

Eftink, M. R., & Jameson, D. M. (1982) *Biochemistry 21*, 4443–4449.

Eftink, M. R., & Selvidge, L. A. (1982) *Biochemistry 21*, 117–125.

Eftink, M. R., & Byström, K. (1986) *Biochemistry* (second of three papers in this issue).

Eftink, M. R., Anusiem, A. C., & Biltonen, R. L. (1983) *Biochemistry 22*, 3884–3896.

Eklund, H., Nordstrom, B., Zepperzauer, E., Soderlund, G., Ohlsson, I., Boiwe, T., Soderberg, B.-O., Tapia, O., & Brändén, C.-I. (1976) *J. Mol. Biol. 102*, 27–29.

Ghiron, C. A., & Longworth, J. W. (1979) *Biochemistry 18*, 3828–3832.

Gottlieb, Y. Y., & Wahl, P. (1963) *J. Chim. Phys. 60*, 849–856.
Gratton, E., Jameson, D. M., & Hall, R. D. (1984) *Annu. Rev. Biophys. Bioeng. 13*, 105–124.
Grinvald, A., & Steinberg, I. z. (1974) *Biochemistry 13*, 5170–5178.
Hagaman, K., & Eftink, M. R. (1984) *Biophys. Chem.* (in press).
Jameson, D. M., & Gratton, E. (1983) in *New Directions in Molecular Luminescence* (Eastwood, D., Ed.) pp 67–81, American Society for Testing and Materials, Philadelphia, PA.
Jameson, D. M., Gratton, E., & Hall, R. D. (1984) *Appl. Spectrosc. 20*, 55–106.
Knutson, J. R., Walbridge, D. G., & Brand, L. (1982) *Biochemistry 21*, 4671–4679.
Lakowicz, J. R., & Maliwal, B. P. (1985) *Biophys. Chem. 21*, 61–78.
Lakowicz, J. R., Maliwal, B., Cherek, H., & Balter, A. (1983) *Biochemistry 22*, 1741–1752.
Laws, W. R., & Shore, J. D. (1978) *J. Biol. Chem. 253*, 8593–8597.
Maret, W., Andersson, I., Dietrich, H., Schneider-Bernlohr, H., Einarsson, R. & Zeppezauer, M. (1979) *Eur. J. Biochem. 98*, 501–512.
Meech, S. R., Phillips, D., & Lee, A. G. (1983) *Chem. Phys. 80*, 317–328.
Ross, J. B. A., Schmidt, C. J., & Brand, L. (1981) *Biochemistry 20*, 4369–4377.
Saviotti, M. L., & Galley, W. (1974) *Proc. Natl. Acad. Sci. U.S.A. 71*, 4154–4158.
Szabo, A. G., Stepanik, T. M., Wagner, D. M., & Young, N. M. (1983) *Biophys. J. 41*, 233–244.
Theorell, H., & Yonetani, T. (1963) *Biochem. Z. 338*, 537–553.
Theorell, H., & Tatemoto, K. (1971) *Arch. Biochem. Biophys. 142*, 69–82.
Weber, G. (1952) *Biochem. J. 51*, 145–155.
Weber, G. (1981) *J. Phys. Chem. 85*, 949–953.
Weber, G., & Shinitzky, M. (1970) *Proc. Natl. Acad. Sci. U.S.A. 65*, 823.
Wolfe, J. K., Weidig, C. F., Halvorson, H. R., Shore, J. D., Parker, D. M., & Holbrook, J. J. (1977) *J. Biol. Chem. 252*, 433–436.

Oxidation–Reduction Potentials of Butyryl-CoA Dehydrogenase†

Cheri W. Fink, Marian T. Stankovich,* and Sean Soltysik
Department of Chemistry, University of Minnesota, Minneapolis, Minnesota 55455
Received May 1, 1986; Revised Manuscript Received June 30, 1986

ABSTRACT: In order to obtain butyryl-CoA dehydrogenase from *Megasphaera elsdenii* in pure enough form to perform redox studies, the existing purification procedures first had to be modified and clarified [Engel, P. (1981) *Methods Enzymol. 71*, 359–366]. These modifications are described, and the previously unpublished spectral properties of the electrophoretically pure CoA-free butyryl-CoA dehydrogenase are presented. In our spectral reductive titration of pure enzyme, we show that although blue neutral flavin radical is stabilized in nonquantitative amounts in dithionite titrations (19%) or in electrochemical reductions mediated by methylviologen (5%), it is not thermodynamically stabilized; therefore, only a midpoint potential for butyryl-CoA dehydrogenase is obtained. The electron-transfer behavior from pH 5.5 to pH 7.0 indicates reversible two-electron transfer accompanied by one proton:

$$EFl_{ox} + 2e^- + H^+ = EFl_{red}H^- \quad E_{m7} = -0.079 \text{ V vs. SHE}$$

where EFl_{ox} is oxidized butyryl-CoA dehydrogenase, $EFl_{red}H^-$ is two electron reduced enzyme, and E_{m7} is the midpoint potential at pH 7.0 at 25 °C. Redox data and activity data both indicate that the enzyme loses activity rapidly at pH values above 7.0. The E_{m7} of the butyryl-CoA dehydrogenase is 40 mV positive of the E_{m7} of the butyryl-CoA/crotonyl-CoA couple [Gustafson, W. G., Feinberg, B. A., & McFarland, J. T. (1986) *J. Biol. Chem. 261*, 7733–7741]. Binding of substrate analogue acetoacetyl-CoA caused the potential of butyryl-CoA dehydrogenase to shift 100 mV negative of the free enzyme. The negative shift in potential makes electron transfer from enzyme to substrate more probable, which is consistent with the direction of electron transfer in the bacterial system. Our work suggests that substrate binding may cause the potentials of the mammalian and bacterial fatty acyl-CoA dehydrogenases to shift in different directions in accord with the opposing directions of electron transfer in the two kinds of organisms.

Butyryl-CoA dehydrogenase (EC 1.3.99.2) from *Megasphaera elsdenii* catalyzes the two electron transfer reaction in fatty acid metabolism shown below. The substrates in the

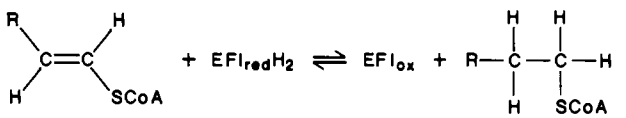

reaction are the same as for the mammalian system, but the direction of the electron transfer is reversed, with the bacterial

† This work was supported by a grant from the National Institutes of Health (GM 29344).
* Author to whom correspondence should be addressed.

0006-2960/86/0425-6637$01.50/0